

Parametric Analysis to Support the Integrated Design and Performance Modeling of Net-Zero Energy Houses

William O'Brien

Student Member ASHRAE

Andreas Athienitis, Ph.D., P.Eng

Member ASHRAE

Ted Kesik, Ph.D, P.Eng

Member ASHRAE

ABSTRACT

Building performance models routinely involve tens or hundreds of components or aspects and at least as many parameters to describe them. This results in overwhelming complexity and a tedious process if the designer attempts to perform parametric analysis in an attempt to optimize the design. Traditionally, during design, parameters are selected on a one-at-a-time basis, and occasionally, formal mathematical optimization is applied. However, many subsets of parameters show some level of interaction – to varying degrees – suggesting that the designer should consider manipulating multiple design parameters simultaneously. This paper is divided into two parts. The first part presents a methodology for identifying the critical parameters and two-way parameter interactions. The second part uses these results to identify the appropriate level of modeling resolution. The methodology is applied to a generic model for net-zero or near net-zero energy houses, which will be used for an early stage design tool. The results show that performance is particularly sensitive to internal gains, window sizes, and temperature setpoints and they indicate the points at which adding insulation to various surfaces has minimal impact on performance. The most significant parameter interactions are those between major geometrical parameters and operating conditions. Increased modeling resolution for infiltration and building-integrated photovoltaics (BIPV) only provides a modest improvement to simpler models. However, explicit modeling of windows, rather than grouping them into an equivalent area, has a significant impact on predicted performance. This suggests that identifying and implementing the appropriate level of modeling resolution is necessary, and that it should be detailed for some aspects even in the early stage design.

INTRODUCTION

Currently, net-zero energy buildings (NZEBs) are being cited as an effective solution to pending environmental issues (Griffith et al. 2007). NZEBs are frequently defined as buildings that export as much energy as they import over the course of a year; though other definitions exist (Torcellini et al. 2006). Two possible approaches to achieving strong NZEB designs are: formal mathematical optimization and simulation-supported design, in which a designer is involved in every decision. The focus of this paper is early stage design using performance simulation. Put simply, optimization tools output the optimal design based on an objective function and a set of constraints, offering little insight to what makes a good design. Design tools can provide the means to a designer to explore different concepts and reach the near-optimal design space while accounting for their experience and preferences. Unlike formal optimization, design permits the evaluation of unquantifiable design traits such as aesthetics and views to the outside. However, users of design tools are unlikely to arrive at the mathematically absolute optimal solution for large design spaces; though they may come close.

To put the current work in context, a software-based solar house design tool – that is referenced throughout this paper - is being developed for the early stage design. It will support the design of low-energy and net-zero energy houses that include passive solar, active solar, and energy efficiency features. The solar house design tool will replicate what only the most patient of designers would do naturally: support concept generation with a series of proper calculations and simulations through many different design options. The tool should manage issues such as appropriate parameter interactions, design resolution, and modeling assumptions to ensure good results from inexperienced energy modelers.

Currently, common design practice of solar homes involves the expertise of multiple practitioners and at least as many building energy simulation programs – some of which may be custom-built or modified. However, the savings potential (energy and cost) for small residential buildings on an individual basis does not justify this type of investment for mainstream deployment. Thus, there is a need for a streamlined procedure that reduces the level of expertise, design time, and number of distinct information sources (CAD programs, textbooks, design guides, etc.). The absence of such a tool has hindered the widespread adoption of systematic passive solar design in residential buildings. This gap was identified by Athienitis et al (2006) and in the design of several of the Canada Mortgage and

Housing Corporation's EQuilibrium demonstration homes (CMHC 2009). It should be noted that the use of thorough design and simulation is particularly justified for prefabricated homes or subdivisions in which a large number of houses is similar or identical.

The biggest challenge in designing a low- or net-zero energy house, as with any engineering system, is that the designer must make multiple design decisions simultaneously with the goal of achieving a high level of performance. The process is not as simple as merely selecting the best choice for multiple subsystems and assuming that this will yield the best system upon integration. In reality, each subsystem interacts with the others, to some degree. For example, the optimal south-facing glazing area for a passive solar house depends on many other design decisions, including the level of thermal mass and insulation, as well as the control of solar gains and the space heating strategy.

A frequently-cited technique for design is parametric or sensitivity analysis (Hayter et al. 2001). A major limitation to this method is that parameter interactions are overlooked. For instance, the parametric analysis might be performed on a parameter, during which, the other parameters are set to values that do not allow it to be properly characterized. A more concrete example is the interaction between thermal mass and glazing area. A house with minimal glazing and relatively constant operating conditions would indicate little benefit in performance with the addition of thermal mass. Using a single dimensional parametric analysis, an inexperienced designer might make the generalized conclusion that thermal mass has minimal benefit for all buildings. Thus, a methodology for quantifying the significance of parameter interactions is needed.

The focus of this paper is on passive elements of the house, though active solar energy collection is a necessary aspect of NZEBs. The paper includes the description of generic model intended for passive solar houses, a one-dimensional parametric analysis, a two-way interaction analysis, discussion about subsystem interactions, and finally, an in-depth analysis about modeling resolution for three model aspects.

MODEL DESCRIPTION

The underlying model is a rectangular, four-zone house (represented in Figure 1). The purpose of having two above-grade occupied zones is to characterize the possibility of overheating in the direct gain (south) zone. O'Brien et al (2010) showed that performance is relatively sensitive to zonal configuration for passive solar houses. The model was selected to maximize design flexibility, even if some of the parameters and their ranges differ from traditional rules of thumb for passive solar buildings (though they are constrained to adhere to the Model National

Energy Code for Buildings (MNECB) (NRCC 1997)). In the context of the design tool, this design flexibility enables the user to understand all extremes: poor and excellent designs.

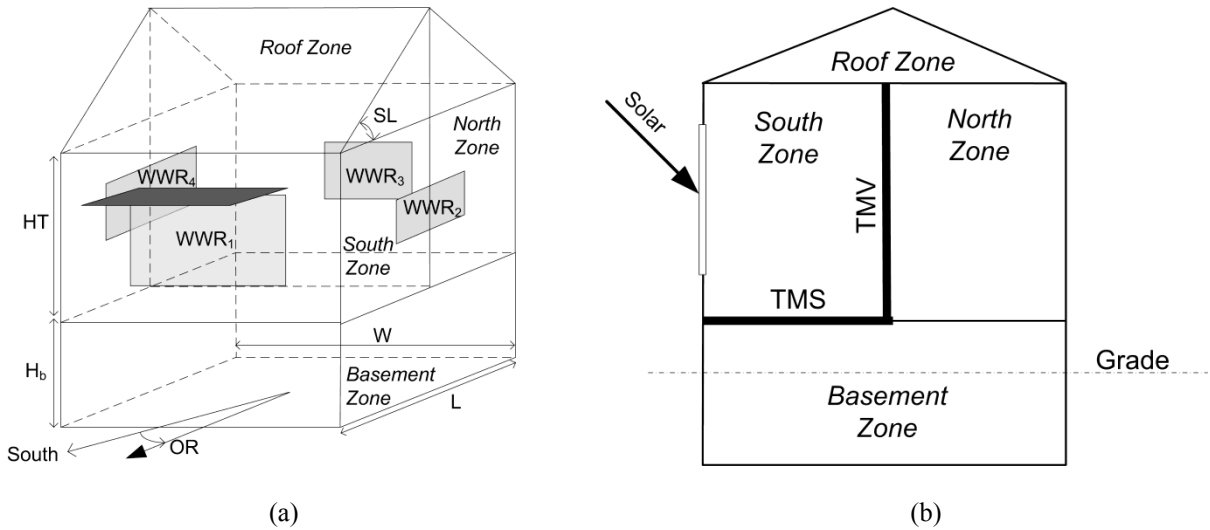


Figure 1. (a) Isometric view of model and (b) East section view of model. Geometry-related parameters are marked on the drawings.

In all, the form, fabric, controls, and operations are defined by 30 parameters, as listed in Table 1. These were selected as the most influential subset of a larger group of original parameters.

Table 1. List of Model Parameters and Corresponding Values

No.	Abr.	Name	Definition	Min	Max	Nominal Unit	Design?	Discrete?
1	IN	Infiltration rate	Air infiltration rate (constant)	0.025	0.075	0.1 ach	0	0
2	IG	Internal Gains	Internal (sensible) heat gains scheme	1	3	2 Class number ¹	0	0
3	HS	Heating Setpoint	Minimum temperature to which zones are controlled during the day (7AM to 10PM)	16 (63)	22 (72)	22 (72) °C (°F)	0	0
4	HSN	Nighttime Heating Setpoint	Minimum temperature to which zones are controlled at night (10PM to 7AM)	17 (63)	22 (72)	18 (64) °C (°F)	0	0
5	CS	Cooling Setpoint	Maximum temperature to which zones are controlled during the cooling season	22.5 (73)	27 (81)	26 (79) °C (°F)	0	0
6	FA	Floor Area	Total conditioned floor area (including basement)	100 (1076)	300 (3228)	200 (2152) m ² (sq. ft)	0	0
7	ST	Stories	Number of stories excluding basement	1	2	2 1	0	0
8	AR	Aspect Ratio	Width (oriented nearest to E-W) to Length (oriented nearest to N-S) ratio (assumed)	0.5	2	1 1	1	0
9	OR	Orientation	House orientation; Angle between Wall 1 normal and South (+ = CCW)	-45	45	0 degrees	1	0
10	WR	Wall Resistance	Thermal resistance of all above-grade (opaque) walls from surface to surface	4.4 (25)	12 (68.1)	6 (34.1) m ² K/W (h·ft ² ·°F/Btu)	1	0
11	CR	Ceiling Resistance	Thermal resistance of the ceiling from surface to surface	8.8 (50)	15 (85.2)	10 (56.8) m ² K/W (h·ft ² ·°F/Btu)	1	0
12	BS	Basement Slab Resistance	Thermal resistance of all basement slab (or slab on grade) from surface to surface	1.6 (9.1)	3 (17)	1.6 (9.1) m ² K/W (h·ft ² ·°F/Btu)	1	0
13	BW	Basement Wall Resistance	Thermal resistance of all basement wall from surface to surface	3.1 (17.6)	6 (34.1)	3.1 (17.6) m ² K/W (h·ft ² ·°F/Btu)	1	0
14	WT1	Window Type 1	Type of window for South-most window(s)	1	5	3 Class number ²	1	1
15	WT2	Window Type 2	Type of window for East-most window(s)	1	5	3 Class number ²	1	1
16	WT3	Window Type 3	Type of window for North-most window(s)	1	5	3 Class number ²	1	1
17	WT4	Window Type 4	Type of window for West-most window(s)	1	5	3 Class number ²	1	1
18	FT	Frame Type	Frame type for all windows on house	1	3	2 Class number ³	1	1
19	WWR1	Window-to-Wall Ratio 1	Window-to-wall ratio for South-most window(s)	0.05	0.8	0.4 1	1	0
20	WWR2	Window-to-Wall Ratio 2	Window-to-wall ratio for East-most window(s)	0.05	0.5	0.1 1	1	0
21	WWR3	Window-to-Wall Ratio 3	Window-to-wall ratio for North-most window(s)	0.05	0.5	0.1 1	1	0
22	WWR4	Window-to-Wall Ratio 4	Window-to-wall ratio for West-most window(s)	0.05	0.5	0.1 1	1	0
23	CI	Air circulation rate	Air circulation rate between zones (assumed constant while on); turned on if ΔT>3°C	0	400 (847)	200 (423) L/s (CFM)	1	0
24	OH	Overhang Depth	Overhang depth to window height ratio	0.001	0.5	0.3 1	1	0
25	BLS	Shades close solar threshold	Blinds/shades are closed if both of these conditions are exceeded	0	1000 (317)	150 W/m ² (Btu/h·ft ²) (47.5)	1	0
26	BLT	Shades close temperature threshold		15 (59)	40 (104)	20 (68) °C (°F)	1	0
27	TMS	Thermal Mass on South zone floor	Thickness of concrete on on South zone floor	0.001 (0.003 0)	0.2 (0.61)	0.1 (0.31) m (ft)	1	0
28	TMV	Thermal mass on vertical wall	Thickness of concrete on interior vertical surface	0.001 (0.003 0)	0.2 (0.61)	0.1 (0.31) m (ft)	1	0
29	RT	Roof Type	Roof typology	1	2	1 Class number ⁴	1	1
30	SL	Roof Slope	Slope of South-most facing roof (0° = flat)	10	60	35 degrees	1	0

¹ Low, medium, or high internal gains scheme, averaging 550, 850, and 1250 Watts

² Double-glazed, clear, air-filled; double-glazed, clear, argon-filled; double-glazed, low-e, argon-filled; triple-glazed, clear, argon-filled; triple-glazed, low-e, argon-filled

³ Vinyl, wood, or Aluminum with a thermal break

⁴ Gable or hip roof

Each parameter can be classified as *design* or *non-design*. The non-design parameters are defined as those that affect the service that the building provides, namely, shelter, space, and protection from the elements. Put differently,

they are likely to be fixed at the beginning of the design process. The design parameters are defined as those that affect energy performance, but not the service to the occupants.

Continuous parameters can be set to any value within the permissible range (though they may not all be convenient with regards to available building materials). *Discrete* parameters can take on one of a finite set of values. For instance the most appropriate way to define different glazing types is to explicitly model them, rather than having variable optical and thermal properties, since some combinations of which would not be possible (e.g., high transmittance and low U-value).

The parameters were selected to be designer-friendly. For example, instead of defining the major dimensions as length and width, the house's floor area and aspect ratio are used. The reason for this is that the floor space is likely to be fixed (to suit the needs of the occupants), while the aspect ratio may be flexible, depending on building lot constraints.

The nominal settings, denoted in Table 1, were selected to be representative of a good passive solar house design; rather than average values within the range. Unless otherwise noted, the model uses these values except for the parameters that are being explored.

The house was assumed to be occupied between 6PM and 8AM by a family of four. Fresh air was introduced to meet minimum requirements according to (ASHRAE 2004) using a heat recovery ventilator (HRV) with an effectiveness of 60%. Infiltration (*IN*) in the nominal model was modeled at a fixed rate in air changes/hour (ach). The effect of a more advanced infiltration model is examined in a later section.

Temperatures were controlled using ideal controls and equipment, in which heat was added or removed from the zones at a rate required to maintain the zone air temperature within the temperature control setpoints. In this way, the heating and cooling energy are determined. Heating was allowed year-round, while cooling was allowed from May 1 to September 30, representing the typical cooling season for Toronto (the location for which the simulations were performed). The heating setpoint (*HS*) was defined during two control periods per day: day (7 AM to 10 PM) and night (the remainder of the day).

Windows were modeled by grouping all windows on each surface as a single window and with a frame that surrounds them. Windows were assumed to be congruent to, and centered within, their parent surfaces. The effect of explicitly modeling individual windows (instead of grouping them) is examined in a later section.

Several strategies were implemented to minimize overheating and improve thermal comfort, including: an overhang over the south-facing window, actively controlled interior Venetian blinds, free cooling, and enhanced zone air mixing. Overhangs for the non-south facing windows were found to be ineffective because they are poor at obstructing the summertime sun. The overhang over the south-facing window was positioned just high enough such that it never shades the glazing at winter solstice. The overhang parameter (OH) defines the depth of the overhang relative to the glazing height. The controlled Venetian blinds were assumed to be automatically closed if both the thresholds for outdoor temperature (BLT) and solar radiation on the south-facing window (BLS) are met or exceeded. The free cooling strategy is operated if the zone is overheating and the outdoor air temperature is above 15°C but below the zone air temperature. This could represent natural ventilation or mechanically driven air movement. Explicit natural ventilation through the use of an airflow network was not implemented because the model is intended for early design when little is known about internal airflow pathways. Finally, the CI parameter defines the airflow rate that was used to mix air between zones. This has been found to be effective at distributing solar gains from the direct gain (south) zone to the other zones (O'Brien et al. 2010). It has the benefits of reducing overall heating energy, utilizing thermal mass throughout the house, and increasing overall thermal comfort.

EnergyPlus (US DOE 2009) was selected as the simulation engine for this work because of its extensive modeling capabilities, multiple levels of modeling resolution, and the ease with which it can be scripted to automate the parametric analyses. For all results herein, simulations were performed for Toronto, Canada (Zone 6; latitude: 43.7°N) – a climate with warm, humid summers and cold winters.

ONE-DIMENSIONAL PARAMETRIC ANALYSIS

To quantify the relative significance of the parameters, a main effects plot was created. This has the purpose of identifying the effect of each parameter on energy consumption. All parameters were kept at their nominal values, as listed in Table 1, except for the parameter of interest, which was incrementally simulated to determine the trends over the parameter range. It is important to note that the apparent sensitivity of a parameter is highly-dependent on the range, and must be taken into context when interpreting relative sensitivity (Hui 1998). Figure 2 summarizes the results of the analysis and shows the complete range of simulated performance values for each parameter. Table 2 quantifies the minimum and maximum energy use values and the corresponding parameter values. Parameter

$\text{value}|_{E\min}$ and $\text{value}|_{E\max}$ represent the parameter values at which the minimum heating and cooling energy occur.

Table 2 also quantifies the sensitivity of each parameter according to the following equation (Hui 1998).

$$\left(\frac{\Delta OP}{\Delta IP} \right) \div \left(\frac{\overline{OP}}{\overline{IP}} \right) \quad (1)$$

where ΔOP is the difference in output values (predicted energy use) for the extreme values of each parameter, ΔIP is the difference in input values (extreme parameter values), and \overline{OP} and \overline{IP} are the mean output and input values, respectively.

To provide a more in-depth look into the behavior of the model, four additional graphs shown in Figure 3.

These are particularly important for the parameters that exhibit non-linear curves.

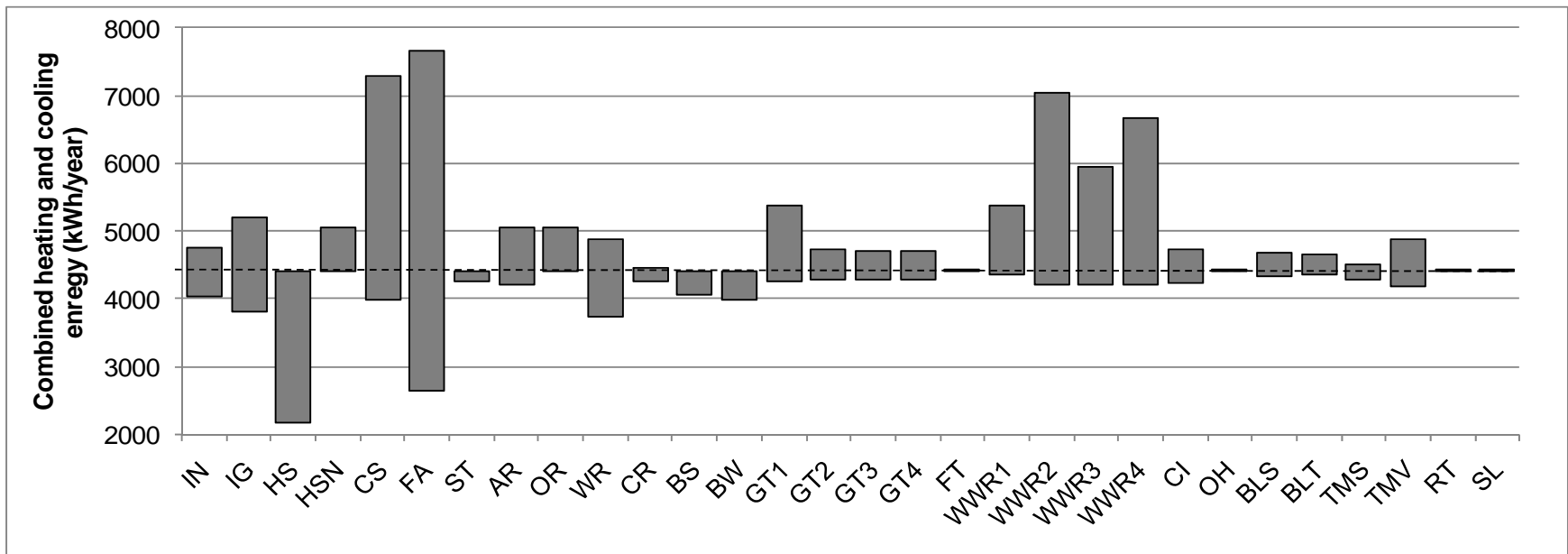


Figure 2. Energy use ranges for 30 parameters. The dashed horizontal line is the energy use when all parameters are at their nominal values.

Table 2. Summary of Sensitivity Analysis for 30 Parameters

	IN	IG	HS	HSN	CS	FA	ST	AR	OR	WR	CR	BS	BW	GT1	GT2
Min. Energy (kWh/year)	4042	3801	2172	4394	3991	2637	4251	4209	4403	3724	4253	4058	3972	4264	4288
Max. Energy (kWh/year)	4766	5203	4403	5059	7300	7660	4403	5045	5061	4874	4460	4403	4403	5377	4717
Parameter value _{Emin}	0.025	3	16	17	22.5	100	1	1.85	0	12	15	3	6	5	5
Parameter value _{Emax}	0.075	1	22	22	27	300	2	0.5	-45	4.4	8.8	1.6	3.1	1	1
Parameter unit	ach	-	°C	°C	°C	m ²	m	-	degrees	m ² K/W	m ² K/W	m ² K/W	m ² K/W	-	-
Sensitivity	0.1646	-0.627	2.4601	0.5664	3.4494	1.0704	-0.052	0.1579	1E-07	0.3001	0.0915	0.135	0.1634	-0.698	-0.285
	GT3	GT4	FT	WWR1	WWR2	WWR3	WWR4	CI	OH	BLS	BLT	TMS	TMV	RT	SL
Min. Energy (kWh/year)	4292	4290	4403	4362	4216	4209	4199	4240	4399	4328	4367	4289	4170	4402	4397
Max. Energy (kWh/year)	4717	4717	4418	5381	7046	5959	6662	4721	4439	4667	4665	4507	4871	4403	4418
Parameter value _{Emin}	5	5	2	0.5	0.05	0.05	0.05	400	0.3503	0	19	0.2	0.2	2	50
Parameter value _{Emax}	1	1	1	0.05	0.5	0.5	0.5	0	0.001	1000	40	0.001	0.001	1	10
Parameter unit	-	-	-	-	-	-	-	L/s	-	W/m ²	°C	m	m	-	degrees
Sensitivity	-0.283	-0.284	-0.007	0.1251	0.3162	0.2109	0.2824	0.0543	0.0045	0.037	0.0547	0.0252	0.0796	-4E-04	0.0032

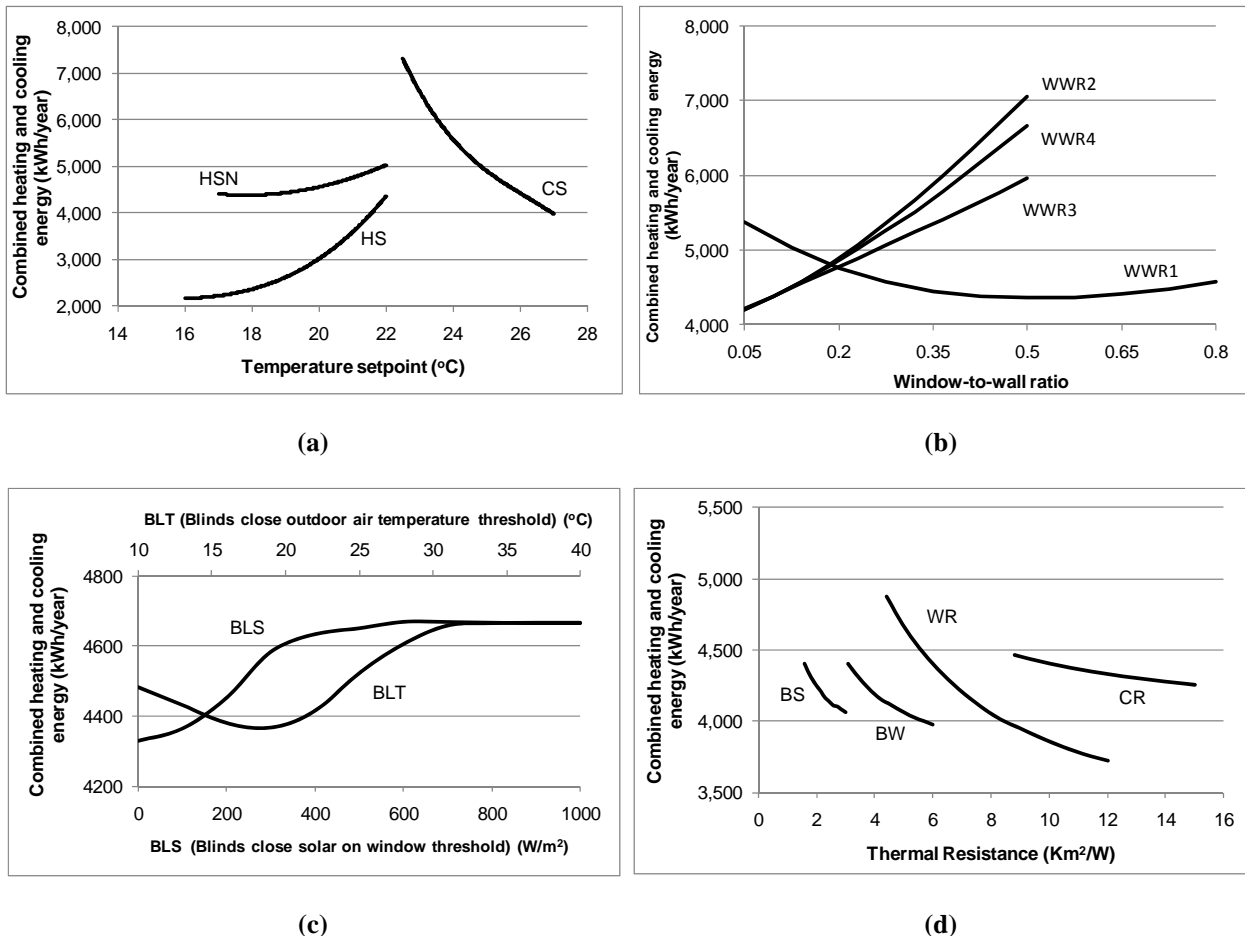


Figure 3. Select sensitivity analyses, as simulated at in increments of tenths of the total parameter range. (a) temperature setpoints, (b) window-to-wall ratios, (c) control setpoints for blind closer, and (d) insulation levels in opaque constructions.

The most significant parameters are those that define the operations of the house, followed by those that define the house's major geometrical properties and windows.

Infiltration plays an important role in performance predictions that is comparable to parameters with more certainty such as insulation. This is primarily because heat loss and gains (in summer) from infiltration can rival heat transfer through the relatively well-insulated envelope. This indicates a strong need for careful estimation and modeling of infiltration. However, the only accurate way to determine a house's infiltration characteristics is with a blower door test (ASHRAE 2005). Yet, this can only be performed after construction. This issue is addressed in a later section. Similarly, the combined heating and cooling energy use is sensitivity to the internal gains from non-HVAC loads and people. This demonstrates the importance of estimating a reasonable value and introducing measures to reduce the value early in design, using daylighting, low-energy appliances, and advanced controls, such as occupancy controls for ventilation and lighting.

Results are quite sensitive to heating and cooling setpoints, as indicated by Figure 3a. This is partly owing to the fact that if the temperature is allowed to float within a larger temperature range, the temperature difference across the envelope will be lower on average, translating to less conductive heat transfer. Similarly, infiltration heat losses are lower under a smaller temperature difference. However, more importantly, a larger temperature range enables greater storage of solar gains. By definition, no sensible energy can be passively stored without an increase in temperature in zone air and the surrounding surfaces. Thus, the performance is particularly sensitive to setpoints for passive solar houses. This result emphasizes the fact that if occupants can adapt to larger temperature swings, the house's purchased energy can be significantly lowered.

Floor area was shown to have a significant effect on performance because infiltration and absolute envelope conductance increase with these parameters. The number of stories was shown to have little impact on performance. This is largely a result of the fact that the one-storey design's smaller non-south windows for a given window-to-wall ratio balances out with the larger roof and basement areas. Note that the total floor area is the same regardless of the number of storeys. Since the nominal design parameter settings involve a large glazing area on one of the walls (nominally south) and much smaller ones on the others, performance is relatively sensitive to orientation. The optimal orientation of the largest window was found to be nearly due south, as expected.

Insulation levels – particularly for the above-grade walls – was found to have a moderate impact on performance. The *WR* parameter is the most significant of the insulation parameters simply because the above grade walls are higher in exposed area than the other surface types. The moderate sensitivity to basement insulation indicates a need for accurate ground temperature modeling. All insulation-related parameters are shown to provide diminishing returns, as indicated by Figure 3d.

Glazing types that have a lower thermal conductance at the cost of a lower solar heat gain coefficient (SHGC) value are superior for all orientations. The glazing type for the south-facing window is particularly critical because of its large area.

Results are relatively insensitive to the window frame type. However, as mentioned, the windows on each orientation are grouped into a single equivalent window. This may underestimate the U-value of the window since the window perimeter (and frame area) is expected to increase if the windows are explicitly modeled with more appropriate sizes. This is closely examined in a later section.

Of the window to wall ratios (*WWR1* through *WWR4*), performance only improves when the south-facing window-to-wall ratio was increased; though the maximum benefit is reached at 50%, at which point the net benefit begins to decrease. Large glazing areas on the east and west facades (*WWR2* and *WWR4*, respectively) have the most detrimental impact on energy use because of the combined factors of higher envelope conductance and greater unwanted solar gains (during the cooling season). This trend is clearly illustrated in Figure 3b.

Of the four main parameters that were included to assess different strategies to prevent overheating, the air circulation rate and blind control setpoints were found to be the most significant. The curves for the blind control setpoints (Figure 3c) show a particularly interesting result; indicating that they must be carefully optimized. They have also been previously shown to be significant for thermal comfort for larger glazing areas (O'Brien et al. 2010). An in-depth analysis of the overhang parameter (*OH*) suggest that an overhang is largely redundant to controlled blinds. In fact, the presence of a deep overhang was found to actually increase transmitted solar radiation at times because it can cause the blinds to remain open (because they are controlled to close above a certain threshold).

The addition of thermal mass is quite beneficial. It moderates zone air temperatures and stores thermal energy for as long as a day, thus bridging the gap between sunny days. Interestingly, the thermal mass on the vertical wall was found to be more beneficial than that on the floor in the south zone. An in-depth analysis yielded two reasons for this. First, during the peak heating season when the solar altitude is low, more direct solar radiation is incident on the wall than on the floor; though this will vary for other geometries. Second, in the summer, the controlled shades tended to be lowered to prevent solar gains, thus causing incoming solar gains to become diffuse. Thus, the presence of the thermally massive wall in the summer is as beneficial as the floor, despite higher solar altitudes.

The roof parameters are relatively insignificant to the passive performance of the house, but come into play when the roof is used to actively collect solar energy – a topic that is explored in a later section.

The realization of the one-dimensional sensitivity analysis in the design tool is that a user-selectable subset of the parameters is displayed in the form of a line graph over the entire parameter range. The graphs are normalized so that they can be easily compared to each other. Since the intent of the design tool is to provide fast feedback, the data is generated with from an artificial neural network (ANN), as explained by O'Brien et al (2009). The results of the sensitivity analysis are equally important in determining the factors that must be documented in the “help” documentation of the tool. For instance, it must inform users of how to estimate infiltration, or at least give an

indication of what typical values would be depending on the construction type (e.g., wood frame) and site characteristics (e.g., urban or open field).

While these results are certainly indicative of the sensitivity of performance to each of the parameters, it is important to note that they are dependent on the nominal parameter settings (Lam and Hui 1996). A parameter that would appear to be insignificant from this analysis is not necessarily insignificant in the context of the other parameters. If it exhibits strong interactions with one or more other parameters, then its inclusion is essential. Thus, while it is sometimes suggested that a parameter may be eliminated based on the results of such a sensitivity analysis, this should be exercised with caution. In the next section, this limitation is considered by examining all two-way interactions between the parameters.

PARAMETER INTERACTIONS

As mentioned, it would be unwise to merely optimize each parameter independently since they all interact to some level. For instance, O'Brien et al (2008) showed that the optimal south-facing glazing area for house with high internal gains was a third of the size of the optimal size with minimal internal gains. Therefore, one can conclude that certain parameters should be manipulated in subsets, rather than individually. Obviously, manipulating more than several parameters simultaneously is tedious and yields an exponentially expanding design space. To solve this problem, simulations were run to identify the most significant interactions between pairs of parameters.

For a population of 30 parameters, there are 435 (30 choose 2) two-way interactions to consider. The focus of this work is on two-way interactions since high-order interactions are unusual (Shah et al. 2000). One commonly used method to understand interactions is to create interactions plots, as is commonly performed in the field of design of experiments (DOE) (Mason et al. 2003). In all, 435 plots were created using MATLAB to drive EnergyPlus simulations with specific values of the 30 parameters. For the plots, all parameter settings were set to the nominal values (as previously defined), except for the pair of parameters being examined. For those two parameters, the extreme values were combined, to yield four (2^2) different parameter combinations and corresponding performance values. Thus, for the 435 pairs of parameters, 1740 simulations were run.

Once the values (in this case combined annual heating and cooling energy) were obtained from the simulation results; they were plotted. The two parameters are denoted *A* and *B* herein. Each interactions plot contains two lines,

each indicating a different value for parameter B , as shown in Figure 5. The endpoints of each line correspond to the low (left) and high (right) values of parameter A. It is important to note that these lines no not necessarily indicate a linear relationship between performance and the parameter value; they appear as linear because only the extreme parameters are evaluated (rather than the midpoints) for the interactions analysis. If the lines are parallel, this indicates that there is no interaction between the two parameters. In contrast, if they are nonparallel, an interaction exists. The relative slope of the lines indicates the magnitude of the interaction. The standard method for quantifying the interaction is using equations 1, 2 and 3 (Mason et al. 2003).

$$E_{A,B(-1)} = R_{A(-1)B(-1)} - R_{A(+1)B(-1)} \quad (2)$$

$$E_{A,B(+1)} = R_{A(-1)B(+1)} - R_{A(+1)B(+1)} \quad (3)$$

$$I_{A,B} = 0.5(E_{A,B(+1)} - E_{A,B(-1)}) \quad (4)$$

where A and B are the two parameters being examined for interactions, $I_{A,B}$ is the magnitude of the interaction, $E_{A,B(+1)}$ is the effect of parameter A at the high level of parameter B , and $E_{A,B(-1)}$ is the effect of parameter A at the low level of parameter B , and the R_{AB} terms are the response (heating and cooling energy for this application) depending on the values of A and B . The responses (R_{AB}) are shown in Figure 4.

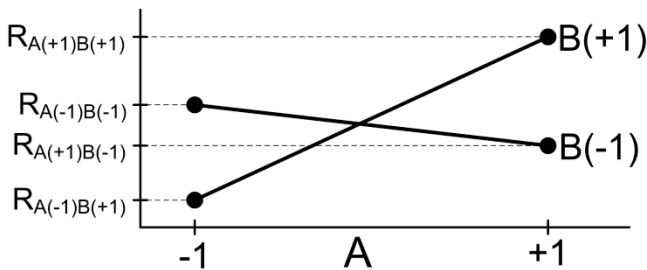


Figure 4. Generic representation of responses and interactions

The principle is best explained with two examples. Figure 5a shows the interaction between the south-facing glazing area (WWR_1) and type (GT_1); representing the single strongest interaction between two design parameters. In practical terms, this means the window area and type should not be selected independently because the optimal glazing area is dependent on the glazing type. The results show that a large glazing area is beneficial if it is triple-glazed, low-e, argon-filled. However, total energy use actually increases under the same range of glazing areas for clear, double-glazed, air-filled windows. Thus, clearly a designer who attempts to optimize one parameter at a time would oversee this critical interaction.

A very important observation from Figure 5a is that the two points corresponding to low *WWRI* values are nearly coincident, despite the other parameter (*GTI*) being at its two extremes. While the results are intuitive in this case, it proves that one-dimensional parametric analyses can overlook the significance of parameters.

In contrast, Figure 5b shows minimal interaction between the wall and ceiling thermal resistance (*WR* and *CR*). It indicates that if either of these quantities is increased individually, the energy use decreases, and that, regardless of the value of *WR*, increasing *CR* is beneficial (for the range of values that were explored).

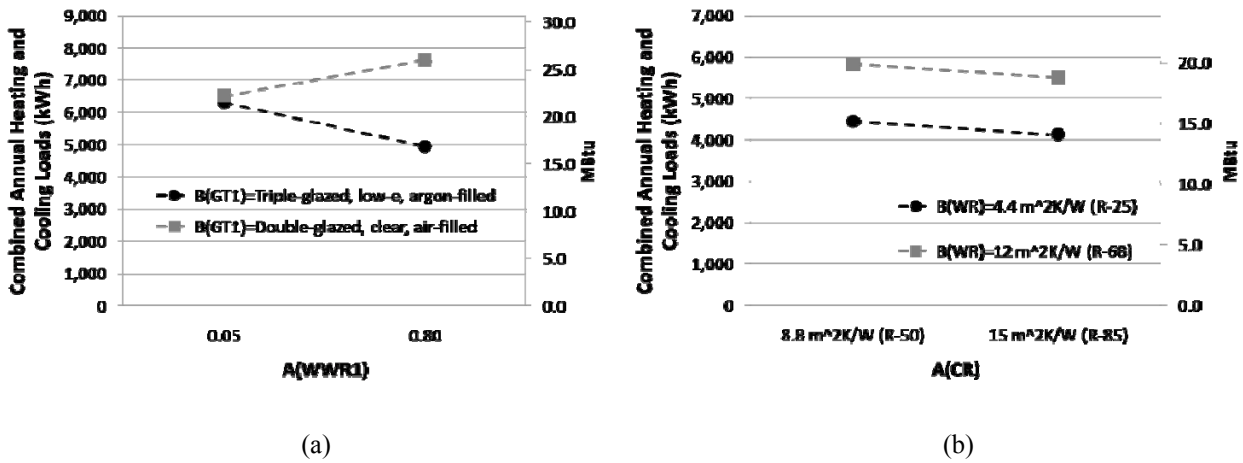


Figure 5. Example interactions plots showing (a) a strong interaction and (b) a weak interaction.

The interactions are shown using an “interactions wheel” in which the parameters are plotted around a circle and those joined by a line indicate that their strength. Figure 6 shows an example in which the strength of interaction between south-facing window-to-wall ratio (*WWRI*) and the other parameters are displayed. The line thicknesses are proportional to the magnitude of the interactions. This visualization is used in the design tool for a single user-selectable parameter so that they can immediately understand which other (highly-interacting) parameters they should be concerned with at that moment. This can give the user peace of mind for whether or not the change of a parameter has a significant impact on the design, in a design space that the most insightful of users will recognize as being complex.

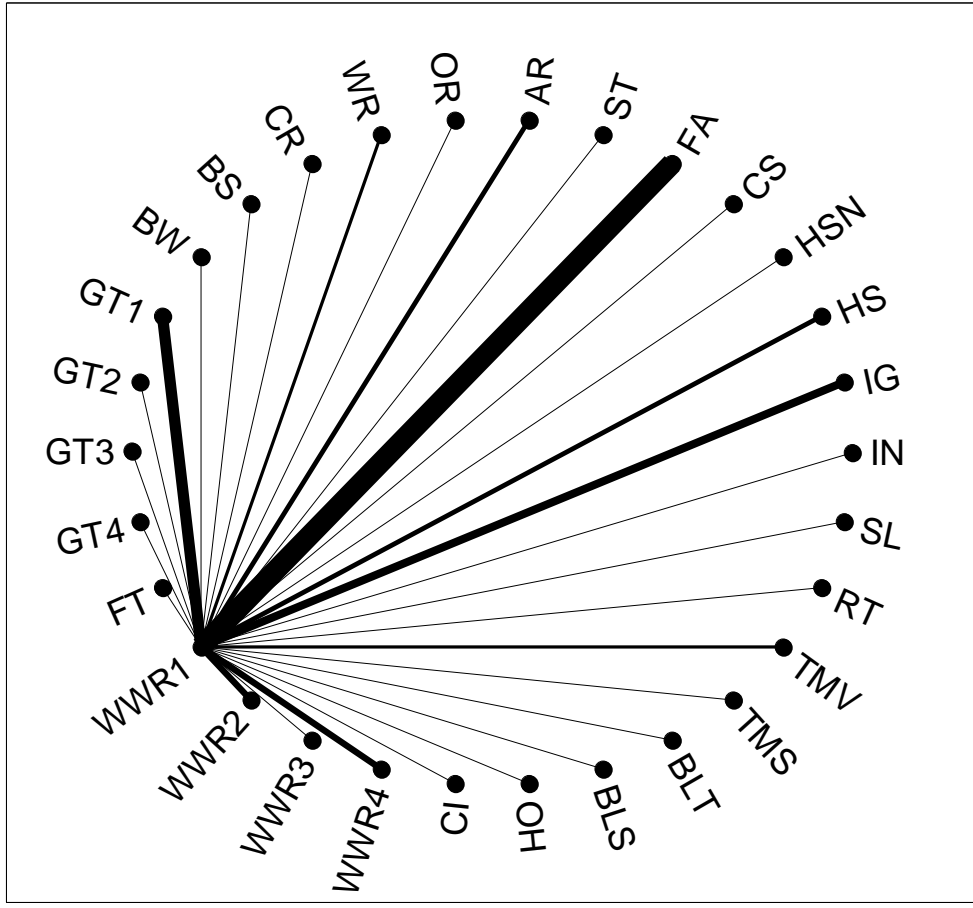


Figure 6. Visualization of the interactions with WWR1. Each line connecting two parameters indicates a strong interaction. The line thickness is proportional to the strength of the interaction.

Interactions between two design parameters are important because those are of most interest to the designer. While some, such as the one in Figure 5a is intuitive, others are less so, such as that between GT_1 and AR or WR and $WWR1$. These stronger interactions, suggest that the design space should be assessed in a multi-dimensional fashion, where an array of practical combinations is explored. In contrast, parameters that show minimal interactions with any other parameters can be optimized individually; saving significant effort. For instance, as one would expect, the parameters defining the roof have minimal influence on the heating and cooling energy of the house. This freedom means that the roof can be effectively decoupled from the rest of the house and that the roof can be optimized for active solar energy collection.

As previously, explained non-design parameters are those that would be set early in the design process as constraints or assumptions, and are unlikely to be modified later unless additional information is obtained. Thus, the designer may not be concerned with their values when attempting to optimize performance. However, strong

interactions that involve non-design parameters are important, nonetheless. They emphasize the importance of accurately predicting them. For instance, the internal gains scheme (*IG*) exhibits strong interactions with the south-facing glazing areas (*WWR1*). This indicates that properly predicting the non-HVAC, occupant-driven loads is critical to optimizing glazing area. In the context of the design tool, the non-design parameters that exhibit significant interactions with other parameters should be modeled and predicted with as much accuracy as reasonably possible.

The implication of interactions in the design process is that once the strong interactions are identified, then the lesser interactions can be mostly overlooked. The top ten interactions are listed in Table 3 and the top ten interactions involving design parameters only are listed in Table 4. Note that $|I_{A,B}| = |I_{B,A}|$, and thus, absolute values are shown.

Table 3. Top Ten Interacting Pairs of Parameters

Rank	Interacting Parameters (no restrictions)	$I_{A,B}/\max(I_{A,B})$
1	WWR1	FA
2	FA	HS
3	FA	IG
4	WWR1	GT1
5	WWR3	GT3
6	HSN	HS
7	ST	FA
8	WWR4	GT4
9	WWR1	IG
10	WWR2	OR

Table 4. Top Ten Interacting Pairs of Design Parameters

Rank	Interacting Parameters (design parameters)	$I_{A,B}/\max(I_{A,B})$
1	WWR1	GT1
2	WWR3	GT3
3	WWR4	GT4
4	WWR2	OR
5	WWR2	GT2
6	WWR4	OR
7	WWR2	WWR1
8	WWR4	WWR1
9	WWR1	AR
10	GT1	AR

The results indicate that interactions involving window area and other major geometrical parameters are among the most significant. Additionally, operational-based parameters are involved in some very significant interactions. For example, the south-facing window-to-wall ratio (*WWRI*) is highly interacting with the floor area. This is because larger windows are more beneficial to larger houses, which have greater heat losses and a higher capacity to passively store solar gains. The relationship between the glazing types (*GT*) and (*WWR*) represent the strongest interactions among the design parameters because the benefit (or hindrance) of a window is highly-dependent on its thermal and optimal properties. A large south-facing window is only beneficial if it has a sufficiently high solar transmittance and a sufficiently low conductance.

MODEL COUPLING AND DECOUPLING

Interactions are not limited to occurring between parameters, but can also occur between entire subsystems (e.g., photovoltaic arrays, the house's envelope, solar thermal systems, etc.). Subsystems that do not interact at all can be designed independently. However, subsystems with substantial interactions should be designed in an integrated manner because the change of one subsystem is likely to have a significant effect on the other(s). The importance of assessing the level of interaction is evident in reducing design efforts.

Figure 7 qualitatively describes the level of interaction between subsystems using a Venn diagram; with the central subsystem being the house's envelope and associated base loads. Interactions can be performance-based, practical, or thermal, in nature, and are noted in the diagram.

Performance-based interactions are those for which the performance of two subsystems depend on the design of the other. For instance, any solar thermal systems that supplements purchased heating depends on the design of the envelope. An energy efficient envelope will tend to be less dependent on the active solar collectors, and thus, the contribution of the active solar collectors is lessened. Therefore, the solar collectors and storage should be sized for the specific house.

Practical interactions are those in which geometrical or other practical constraints must be considered. For instance, if BIPV roof is to be entirely covered in PV modules, the slope and dimensions of the roof must be selected to accommodate commercially available products. The EcoTerra roof's slope, at 30°, was partly selected so that the PV modules covered the entire distance from the eves to the ridge (Noguchi et al. 2008). If only a practical interaction exists between two subsystems they may be modeled independently as long as the designer ensures

compatibility between them. For instance, EcoTerra's BIPV was modeled separately (and with a different tool) from the thermal performance of the house to exploit the features of the different tools.

Thermal interactions indicate that there is significant thermal coupling between subsystems. For instance, the passive solar performance of a house must be explicitly modeled within the context of the house's envelope. In contrast, despite the fact that BIPV is adhered to a building surface, the solar aperture, for instance, is unlikely to affect PV performance, and vice versa. Thus, the two could be safely modeled separately. The thermal coupling between PV and the building envelope is closely examined in a later section.

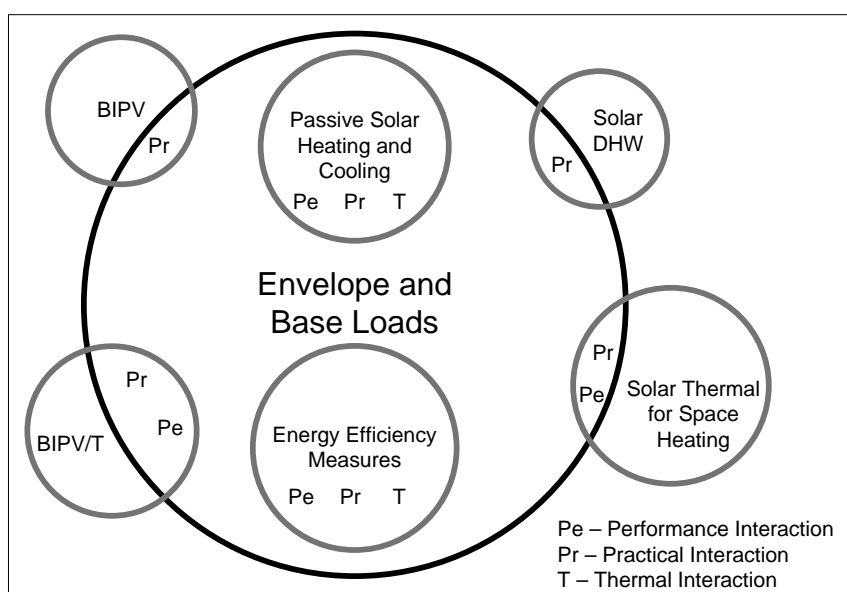


Figure 7. Venn diagram of the potential for decoupling the subsystems. (BIPV = building-integrated photovoltaics; DHW = domestic hot water; BIPV/T = building-integrated photovoltaics with thermal energy recovery)

The best prospects for decoupling from the envelope and base loads are BIPV and solar DHW systems. BIPV's performance is not dependent on energy demands of the house (for grid-tied systems). While PV performance is a function of its operating temperature, this is unlikely to vary significantly between different house designs. Solar DHW systems' performance is dependent on demand. However, demand is not tied to the design of the house, per se, but rather occupant behavior. Both systems do share a geometric relationship with the house, but these relationships can be managed externally to the thermal models.

Solar thermal systems for space heating (including BIPV/T) have some traits in common with the other types of solar collector. However, their performance is tied to demand from the house. If no heat is needed because of passive

solar gains, the system contributes nothing at that time, unless thermal storage is available. Similarly, collector performance may depend on the temperature of the storage medium (for closed loop systems).

Decoupling models not only offers computational advantages, but more importantly, it helps the designer, by breaking the problem into more manageable problems and reduces the number of possible design combinations. Furthermore, it allows the use of multiple design tools in the case where the design tool of choice does not have a certain feature or technology. In the context of the design tool that is currently being developed, the identification of the models that can be decoupled offer advantages: (1) they can use separate models as simulation engines, and (2) they can be simulated independently, which often reduces model complexity and consequently, simulation time. Similarly to the weak interactions between parameters, weak interactions between subsystems can be identified in the “help” documentation as those which can be largely individually optimized.

APPROPRIATE MODEL RESOLUTION

This section examines three significant aspects of the model in varying degrees of modeling resolution to determine their importance. These include infiltration, BIPV, and window modeling. This is critical in the development of the generic model used in the design tool because there is a need to balance resolution with accuracy. The objective of the design tool is to allow the user to focus on design and relieve them of the concern of modeling details.

Infiltration Modeling

Previously, infiltration was shown to be the single most significant factor in predicted performance under the ranges considered. For this reason, it deserves attention and potentially higher model resolution. Yet, as mentioned, a building’s airtightness can only be reasonably determined using a blow door test. Even visual inspection cannot accurately predict airtightness (ASHRAE 2005). For early stage design, little is known about a house’s infiltration characteristics, other than its major geometry and exposure to wind. Thus, this section focuses on two different modeling options, given that the mean air change rate is known.

EnergyPlus can either model infiltration as a fixed rate or have it dependent windspeed, outdoor temperature, house geometry, and exposure. The effective leakage area model is considered because it is suitable for small residential buildings (EnergyPlus 2009). For it, infiltration is defined as follows.

$$Inf = \frac{A_L}{1000} \sqrt{C_S \Delta T + C_W V_{wind}^2} \quad (5)$$

where Inf is the instantaneous infiltration rate in m^3/s , A_L is the effective leakage area in cm^2 , C_S is the stack coefficient, C_W is the wind coefficient, ΔT is the temperature difference across the envelope, and V_{wind} is the windspeed. The coefficients are based on empirical data and are typically provided for different building heights and general categories of wind exposure.

For the nominal house design, with “shelter conditions caused by other buildings across the street” and an effective leakage area of 120 cm^2 (18.6 in.^2), the mean annual infiltration is 0.059 ach under normal conditions, or about 1.2 ach at 50 Pa. Infiltration was assumed to distributed evenly among all zones.

The effect of the infiltration rate varying with time can be determined by comparing the fixed rate model with the effective leakage area model. The reason that timing could have an effect - particular for passive solar houses – is that windspeed tends to be higher during the middle of the day when indoor temperatures are higher and thus, heat losses from infiltration could be higher.

The results of this analysis are shown in Table 5. They indicate that the temporal variation of infiltration rates is much less significant (about 6%) than the mean infiltration rate. Thus, the importance of identifying an appropriate infiltration rate is more important than the model, itself, for predicting the performance of un-built houses.

Table 5. Results from Infiltration Model

Model	Mean Infiltration rate (ach)	Annual Heating Energy, kWh (MBtu)	Annual Cooling Energy, kWh (MBtu)
Fixed rate	0.590	3,144 (10.72)	1,029 (3.51)
Effective Leakage Area	0.590	2,964 (10.11)	1,010 (3.45)

BIPV Modeling

As mentioned above, the decoupling of models offers advantages if it is a reasonable assumption. BIPV is routinely modeled as a distinct system using software such as RETScreen (RETScreen International 2005). The RETScreen PV model assumes that the array is freestanding and convectively cooled from both the front and the back surfaces. However, BIPV is typically only exposed on the front surface, causing it to operate at higher temperatures, unless the back is actively cooled (BIPV/T system). The error associated with decoupling the house from the PV is quantified in this section.

Two PV models are considered, including a simple model and the one-diode model. The simple model merely assumes that a constant fraction of incident solar radiation is converted to electricity. This clearly ignores any diminished performance from higher PV cell temperatures that normally occur under direct sunlight.

The one-diode model considers performance under different temperatures and levels of solar radiation, based on empirical performance (EnergyPlus 2009). This has the advantage that the cell temperature is accounted for and that thermal coupling with the building surface can be modeled. The EnergyPlus model has the option for PV modules to be either thermally coupled or decoupled. Only in the thermally coupled option do the building surface and PV array interact, thermally.

The primary interest for this work is building-integrated photovoltaics (BIPV), however, the decoupled option is examined to quantify the significance of this effect. For the analysis, the Day 4 MC48 module (Day4 Energy 2010), which has a nominal efficiency of about 14.9% and is composed of 48 multicrystalline silicon cells, was considered. It is necessary to model a real module in order to obtain realistic performance characteristics. The roof was modeled with a slope of 35° and south-facing azimuth. Its outer material was dark-colored metal cladding. For the analysis, 42 - 1.3 m² (14 sq. ft) modules were modeled as integrated in a spatially distributed fashion onto the roof, which is equivalent to having 80% of the roof covered in active solar cells.

The use of the simple model used an equivalent PV cell area with equal efficiency to that of the one-diode model under nominal conditions. The one-diode model was explored under decoupled conditions as well as coupled to the roof. Both unvented and vented roofs were examined. The vented roof was assumed to be highly ventilated, at a rate of 100 ach. This is not the same as air-based BIPV/T systems, in which air is passed directly behind the PV modules, increasing the convective heat transfer and removing much of their heat bi-product.

All performance metrics assume that the system is grid-tied and that all generated electricity is useful. Only DC generation was considered to eliminate the effect of inverter losses.

Table 6. PV performance results for different models

Model	Thermal Coupling	Annual DC Generation, kWh (MBtu)	Annual Solar Radiation on Cells, kWh (MBtu)	Mean Efficiency	Peak PV Temperature, °C (°F)	Mean Operating Temperature, °C (°F)
Simple	Decoupled	11,034 (37.6)		14.90%	-	-
One-diode	Decoupled	10,419 (35.6)		14.07%	59.57 (139.2)	9.77 (49.6)
One-diode	Coupled; Roof Unvented	9,915 (33.8)	74,053 (252.7)	13.39%	72.65 (162.8)	12.26 (54.1)
One-diode	Coupled; Roof Vented	9,980 (34.1)		13.48%	69.95 (157.9)	11.85 (53.3)

The results in Table 6 clearly indicate that the simple model over-predicts performance for BIPV. This is because it neglects performance as a function of solar radiation and cell temperature. However, the error associated with this simplification is only about 10%, which is the same order of magnitude as the effect of snow cover, for instance (O'Brien et al. 2009). Similarly, the performance differences occur between the three cases using the one-diode model. However, perhaps more importantly, the predicted peak temperature for thermally coupled models is 13°C (23°F) hotter than that for the decoupled model. This is a concern, as high PV cell temperatures are damaging to their long-term performance (Chow et al. 2003). The mean operating temperature is defined as the time-averaged temperature when the PV has a positive electrical output.

Overall, BIPV represents a reasonable opportunity for the decoupling of subsystems. Clearly, the design of the roof, other than its orientation, has minimal impact on PV performance, as seen by the difference in performance for the last two cases explored. However, if it is decoupled, the PV model should properly account for reduced heat loss from the back surface to characterize higher operating temperatures and the associated performance. The designer should also be able to verify that peak cell temperatures do not exceed maximum rated temperatures, with some safety margin.

Windows Modeling

The parameters related to the windows were previously shown to be among the most significant of the design parameters. The nominal model, as previously described, modeled all windows on each building surface as a single large window, as is standard practice for early stage design when the window dimensions are unknown. Regarding transmitted solar radiation, this assumption affects the distribution of solar radiation on interior surfaces. This is particularly important in passive solar houses where thermal mass is usually positioned to absorb the solar radiation to minimize the amplitude of temperature swings. Since exact positioning of partition walls tends to be unknown, this may be an acceptable limitation for early stage design. Similarly, the predicted daylighting performance is affected by the assumption, since daylighting is highly sensitive to window positions. Purdy and Beausoleil-Morrison (2001) showed that energy performance is insensitive with window position. However, this analysis was applied to a typical Canadian home with smaller windows than would be expected in a passive solar house. Thus, the effect is expected to be more pronounced here.

Another, and likely more significant, consideration to grouping windows is the window conduction. For constant frame widths, a house with smaller windows, but equivalent total glazing area, will have a higher frame-to-glazing ratio. Likewise, the glazing edge area (the area of the glazing that is significantly affected by thermal bridging through the window frame) increases. Thus, a larger window is liable to underestimate conductive heat transfer between the zone and outside. The edge area is defined by a 6.5 cm (2.56 in.) perimeter around the edge of all glazing.

Finally, the grouping of windows could affect how shading from solar obstructions is modeled. Overhangs and reveals are of particular concern. Modeling windows as a grouped window neglects some shading from reveals because the shading area from reveals is proportional to the perimeter of the window. Overhangs further complicate matters. If the roof is relied upon as the sole fixed shading device, then the positioning of the windows relative to the roof is critical. However, if the overhangs are positioned relative to the windows, then the modeler only needs to ensure that the geometrical ratios be maintained. As an example of this, the EcoTerra house uses retractable awnings above the upper south-facing windows, as pictured in Figure 8.



Figure 8: The EcoTerra house, showing retractable awnings above the upper windows.

This section examines two geometrical representations for modeling windows with an equal total glazing area, including:

1. Nominal: windows are grouped as a single window with a frame that extends around its perimeter.
2. Explicit: each window is explicitly modeled. The windows are distributed over the wall in an array of two rows of eight windows the south-facing façade.

Other conditions that were modified from the previously-defined nominal conditions include:

- South-facing glazing was 18.86 m^2 (203 sq. ft) ($\text{WWR}_1 = 0.3773$), which is equivalent to 16 square windows with the properties that are defined in Table 7.

Table 7. Properties of Explicitly Defined Windows

	Area, m^2 (sq. ft) (%)	U-value, $\text{W/m}^2\text{K}$ (Btu/h·ft ² ·°F)	SHGC
Centre of glass	0.914 (9.83) (61.2 %)	1.627 (0.287)	0.715
Edge of glass	0.265 (2.85) (17.8 %)	2.682 (0.472)	
Frame	0.314 (3.38) (21.0 %)	2.270 (0.400)	N/A
Total Window Results	1.49 (10.8) (100 %)	1.950 (0.343)	0.565

- For the grouped windows, the same glazing area was maintained while the edge and frame areas are different to maintain the same edge and frame widths. The grouped windows properties are shown in Table 8.

Table 8. Properties of Grouped Windows

	Area, m^2 (sq. ft) (%)	U-value, $\text{W/m}^2\text{K}$ (Btu/h·ft ² ·°F)	SHGC
Centre of glass	17.7 (190.5) (87.8 %)	1.627 (0.287)	0.715
Edge of glass	1.18 (12.7) (5.9 %)	2.682 (0.472)	
Frame	1.27 (13.7) (6.3 %)	2.270 (0.400)	N/A
Total Window Results	20.15 (216.8) (100 %)	1.729 (0.305)	0.670

- $\text{WWR}_2 = \text{WWR}_4 = 0$
- No movable shading devices
- A reveal with an outside depth of 15 cm (6 in.) from the outer glazing surface

The explicitly modeled windows are square and standardized to regular picture windows (ASHRAE 2005). Frame properties were obtained from Window 6 software (Lawrence Berkeley National Laboratory 2009). It should be noted that the “FullInteriorAndExteriorWithReflections” solar distribution option was used in EnergyPlus, to accurately account for shading and the distribution of transmitted solar distribution. The effect of overhangs was also considered, with the overhang depth to glazing height ratio (OH) was set at 0.3. For each combination of effects, a whole-year simulation was performed, as previously defined. The results are summarized in Figure 9.

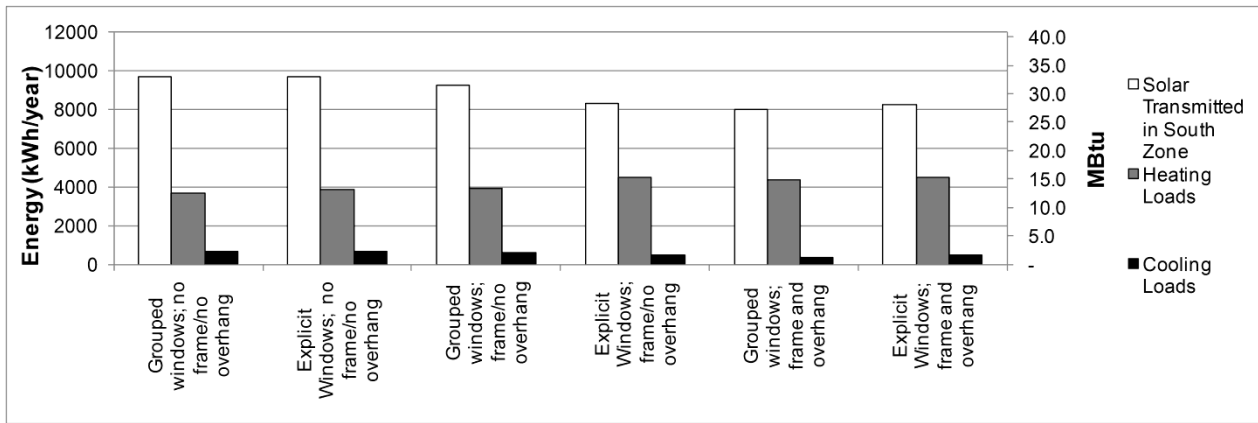


Figure 9: Effect of window modeling resolution.

The results show that transmitted solar energy is at a maximum for the models where no frames, reveals, or overhangs were modeled. As expected, it is nearly equal for grouped and explicitly modeled windows (first two cases in Figure 9). However, the presence of frames and reveals causes the transmitted solar energy to be about 10% less for the explicitly modeled windows relative to the grouped windows. This should be considered very significant. The effect, combined with the higher U-value for the windows (from additional edge and frame area) causes the explicit window case to predict 15% greater heating energy than the nominal case. Cooling declines by about the same fraction; though this has less impact on energy consumption since cooling energy is lower than heating energy. The last two cases in Figure 9 indicate that much of the shading from the reveal(s) occurs from the top of the window, since the presence of an overhang only modestly reduces the amount of transmitted solar energy. While these results are specific to the selected windows, the results demonstrate the relative significance of the modeling resolution of windows.

Interestingly, the explicit windows case took nearly twice as long to simulate (70.66 s) as the grouped window case (37.8 s), although, the apparent improvement in accuracy of predicted performance suggests that this is worthwhile. In the early design stage, rather than attempt to model the exact size window dimensions, it would be appropriate to model typically-sized windows, as was done in this study. The important thing is that the frame effects (both shading and conduction) be reasonably characterized. These results indicate that the design tool that is currently being developed should either explicitly model the windows or if a grouped window is used, its thermal and optical properties should be selected so that the overall performance is equivalent.

CONCLUSIONS

This paper performed an in-depth one- and two-dimensional parametric analysis on a generic passive solar house model that is defined by 30 parameters. The parameters with the greatest influence on predicted energy use are infiltration, internal gains, temperature setpoints, and major geometry parameters. An analysis of all two-way interactions indicated that the most significant interactions involve non-design parameters. The pairs of parameters involved in the strong interactions should be selected simultaneously, while those involved in weak parameters can be safely selected independently.

Entire subsystems also interact to varying degrees. BIPV and solar DHW systems can be modeled independently from the house without introducing significant error, while the systems that reduce purchased heating and/or cooling should be modeled with the house – particularly those that are closed-loop and use thermal storage.

Detailed analyses to determine appropriate modeling resolution for infiltration, BIPV, and windows were performed. The results suggest that predicted performance is particularly sensitive to the way in which windows are modeled. Grouping them into a single area was shown to under-predict energy use by as much as 15%. This suggests that for certain modeling issues, a relatively high level of modeling resolution should be applied – even for early stage design. This should be reflected in the solar house design tool that is being developed.

The issues of parameter interactions, subsystem interactions, and modeling resolution become increasingly more important as houses, and buildings in general, strive to achieve higher levels of performance. This is particularly true for net-zero energy buildings, for which we wish to accurately predict energy demand so that it can be offset with on-site renewable energy collection.

ACKNOWLEDGEMENTS

This work was funded by the Solar Buildings Research Network - a strategic NSERC (Natural Sciences and Engineering Research Council of Canada) research network. Additional support through a grant-in-aid for one of the authors from the American Society of Heating, Refrigeration, and Air-Conditioning Engineers is also acknowledged.

REFERENCES

- ASHRAE 2004. 62.1-2004, Ventilation for acceptable indoor air quality. *American Society of Heating, Refrigerating and Air-Conditioning Engineers, Atlanta.*
- ASHRAE. 2005. *2005 ASHRAE Handbook of Fundamentals:SI Edition*. Atlanga, GA, ASHRAE.
- Athienitis, A. K., Kesik T., et al. 2006. Development of requirements for a solar building design tool. *1st SBRN and SESCI 31st Joint Conference, Montreal, Aug. 20-24, 2006*
- Canada Mortgage and Housing Corporation (CMHC). 2009. The EQuilibrium™ Sustainable Housing Demonstration Initiative. http://www.cmhc.ca/en/inpr/su/eqho/eqho_008.cfm.
- Chow, T., J. Hand and P. Strachan. 2003. Building-integrated photovoltaic and thermal applications in a subtropical hotel building. *Applied thermal engineering* 23(16): 2035-2049.
- Day4 Energy. 2010. 48MC Premium Photovoltaic Modules. <http://www.day4energy.com/downloads/Day4-48MC-Specs-051309-EN.pdf>.
- EnergyPlus. 2009. *EnergyPlus Input/Output Reference*.
- EnergyPlus. 2009. *EnergyPlus Engineering Reference*.
- Griffith, B., N. Long, P. Torcellini, R. Judkoff, D. Crawley and J. Ryan. 2007. Assessment of the Technical Potential for Achieving Net Zero-Energy Buildings in the Commercial Sector. *Golden, CO, National Renewable Energy Laboratory*.
- Hayter, S. J., P. A. Torcellini, R. B. Hayter and R. Judkoff 2001. The energy design process for designing and constructing high-performance buildings. *CLIMA 2000*. Naples, Italy.
- Hui, S. C. M. 1998. Simulation Based Design Tools for Energy Efficient Buildings in Hong Kong
- Lam, J. and S. Hui. 1996. Sensitivity analysis of energy performance of office buildings. *Building and Environment* 31(1): 27-39.
- Lawrence Berkeley National Laboratory 2009. Window 6.
- Mason, R., R. Gunst and J. Hess. 2003. *Statistical design and analysis of experiments: with applications to engineering and science*, Wiley-Interscience.
- National Research Council Canada (NRCC) 1997. Model National Energy Code for Buildings (MNECB). Institute for Research in Construction (IRC): 234.
- Noguchi, M., A. Athienitis, V. Delisle, J. Ayoub and B. Berneche. 2008. Net Zero Energy Homes of the Future: A Case Study of the ÉcoTerra.
- O'Brien, W., A. Athienitis and T. Kesik 2008. Sensitivity Analysis for a Passive Solar House Energy Model. *International Solar Energy Society - Asia Pacific (ISES-AP) Conference Sydney, Australia, Nov. 25-27, 2008*.
- O'Brien, W., A. Athienitis and T. Kesik 2009. The development of solar house design tool. *11th International Building Performance Simulation Association (IBPSA) Conference Glasgow, Scotland, July 27-30, 2009*.
- O'Brien, W., A. Athienitis and T. Kesik 2009. Roofs as extended solar collectors: practical issues and design methodology. *12th Canadian Conference on Building Science and Technology, Montreal, QC, May 6-8, 2009*.
- O'Brien, W., A. K. Athienitis and T. Kesik. 2010. Thermal zoning and interzonal airflow in design of solar houses
Journal of Building Performance Simulation (conditionally accepted).
- Purdy, J. and I. Beausoleil-Morrison 2001. The Significant Factors in Modeling Residential Buildings. *7th International IBPSA Conference, Rio de Janeiro, Brazil*
- RETScreen International. 2005. *Clean Energy Project Analysis*, Ministry of Natural Resources Canada.
- Shah, J. J., S. V. Kulkarni and N. Vargas-Hernandez. 2000. Evaluation of Idea Generation Methods for Conceptual Design: Effectiveness Metrics and Design of Experiments. *Journal of Mechanical Design* 122(4): 377-384.
- Torcellini, P., S. Pless, M. Deru and D. Crawley. 2006. Zero Energy Buildings: A Critical Look at the Definition. *ACEEE Summer Study, Pacific Grove, California*.
- U.S. Department of Energy (US DOE) 2009. Getting started with EnergyPlus, Department of Energy.